

## Localized coastal upwelling at the Brazil Current formation zone (13°S)

Felipe Moraes Santos<sup>1</sup>  
Guilherme Camargo Lessa<sup>2</sup>  
Mauro Cirano<sup>3</sup>  
Ricardo Marques Domingues<sup>4</sup>  
Carlos Alexandre Domingos Lentini<sup>5</sup>

<sup>1</sup> Universidade Federal da Bahia – UFBA/PPGG  
Campus Ondina, Instituto de Geociências - 40.170-020 - Salvador - Bahia, Brasil  
[felipe\\_oceano@yahoo.com.br](mailto:felipe_oceano@yahoo.com.br)

<sup>2,3,5</sup> Universidade Federal da Bahia, Departamento de Oceanografia – UFBA  
Campus Ondina, Instituto de Geociências - 40.170-020 - Salvador - Bahia, Brasil  
[glessa@gmail.com](mailto:glessa@gmail.com); [mauro.cirano@gmail.com](mailto:mauro.cirano@gmail.com); [clentini@ufba.br](mailto:clentini@ufba.br)

<sup>4</sup> Cooperative Institute for Marine and Atmospheric Studies, University of Miami  
Atlantic Oceanographic and Meteorological Laboratory – NOAA  
4301 Rickenbacker Causeway, Miami, FL, 33149, U.S.A.  
[Ricardo.Domingues@noaa.gov](mailto:Ricardo.Domingues@noaa.gov)

**Abstract.** Upwelling events have been investigated for decades on the Brazilian Eastern Margin, with their northernmost occurrence reported at 17°S. This paper has identified, by means of satellite imagery (MODIS) and moored temperature and salinity sensors, 50 coastal upwelling events between 2003 and 2012 centered at 13°S, in the formation zone of both the Brazil Current and the North Brazil Current. Negative temperature anomalies were detected using three different methods that took into account average SST values for the region of study and for defined segments on the shelf. The average negative temperature anomalies varied between -1.0°C and -2.7°C, and were more frequent and stronger in the northern half of the study area. The upwelling events were concurrent with favorable Ekman pumping and Ekman transport, which pumped relatively colder (24°C) and saltier water from water depths between -50 m and -100 m. The upwelled water plumes, that may take the 24°C isotherm as a proxy, had a median surface area of approximately 1,000 km<sup>2</sup>, with the largest plume achieving 5,625 km<sup>2</sup>. The observed negative temperature anomalies and size of the upwelled plumes are smaller than those reported in higher latitudes along the East Brazilian coast. This is ascribed to a thicker mixing surface layer in the region of study.

**Palavras-chave:** Baía de Todos os Santos, remote sensing, sea surface temperature, chlorophyll-a, Bahia

### 1. Introduction

The upwelling of deeper ocean water masses to the surface is a widespread phenomena along eastern boundary currents, but can also be locally witnessed down western boundary currents. One of the western boundary currents where upwelling processes have been intensively investigated is the Brazil Current, which flows from around 13°S to 35°S. The advection of deeper water masses on the Brazilian continental margin has been well documented between 17°S and 24°S, where the upwelling is ascribed to Ekman transport (Aguiar et al., 2014; Castro e Miranda, 1998) and pressure gradients brought on by irregular topographic contours (Palma e Matano, 2009) on the continental margin.

The spatial extension of the upwelling and the temperature anomalies associated with it are about 500 km and -4.5°C at 23°S, respectively. It decreases progressively, however, towards the north where these metrics are 200 km and -2.2°C at 19°S (Melo-Filho, 2006) and 100 km and -1,0 °C at 17°S (Aguiar et al., 2014). Recent evidence from remote sensing

imagery and in situ measurements have indicated that a localized upwelling process takes place at 13°S, in front of Baía de Todos os Santos (BTS) and within the formation zone of the Brazil Current. Therefore, this work aims to report the occurrence of localized upwelling events along the Brazilian shelf at 13°S. To accomplish this, the frequency and seasonal distribution of these events are evaluated along with their area of influence, the wind contribution and their impact on the chlorophyll-a (Chla) concentration.

## 2. Methods

Data on SST and chlorophyll-a concentration (Chla) between 2003 and 2012 were obtained through NASA-MODIS/Aqua (*MODerate-resolution Imaging Spectroradiometer*) from the EOS (*Earth Observing System*) satellite. Daily images Level 1A (L1A – 250m spatial resolution) and 8-day composites Level 3 Mapped (L3 – 4.6 km spatial resolution) were obtained from the NASA website (<http://modis.gsfc.nasa.gov/data/>). MOD28 (Brown et al., 1999) and OC3M (O'Reilly et al., 2000) algorithms were used to process the SST and Chla data (L1A images), respectively. There is, however, no *in situ* measurement or validation for Chla data, and they must be understood as a proxy used to investigate whether upwelled waters enhance coastal productivity in the region of study. The pixels were later resampled to fit a 0.0025° (~275 m) resolution prior to cloud contamination removal.

Additional in situ water temperature and salinity data were acquired from sensors deployed at 33 m of depth at the BTS inlet between May and December 2012 (Figure 1). Wind data was obtained from a National Meteorological Institute weather station (6 hours spacing between 1991 and 2012), from QuikSCAT (daily mean between Jan 2003 and Oct 2009) and from the Cross-Calibrated Multi-Platform Ocean Surface Wind Vector Analysis Fields (CCMP - 5-days mean between Jan 2003 and Dec 2011). The satellite wind data were used to calculate both the Ekman Pumping ( $T_{PUMP}$ ) and Transport ( $T_{EK}$ ).

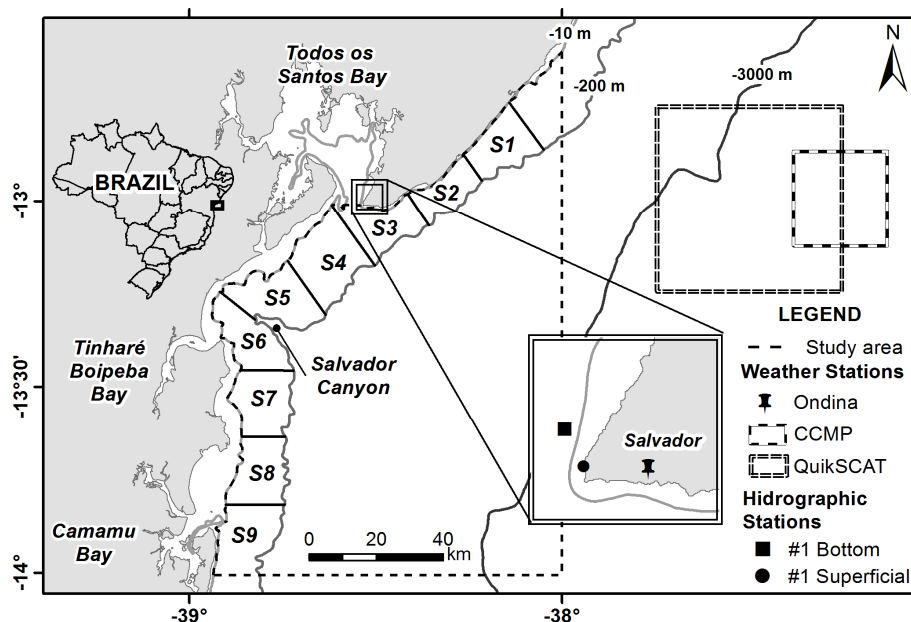


Figure 1: Location of the study area, the segments of the continental shelf and the hydrographic and meteorological stations.

SST gradients from 332 daily images were used for a preliminary identification of the upwelled plumes and measurements of their average alongshore dimension, which was then utilized to subdivide the continental shelf into nine 20 km long segments bounded offshore by the 200 m isobath. The average SST for each of the nine segments, as well as for the study area, were calculated based on 517 8-day composite images

We applied 3 methods to identify the upwelling events: 1) the difference between the daily-average SST for each segment and the respective month-mean of the whole image; 2) the difference between the daily-average SST for each segment and its respective month-mean; 3) the difference between the daily-average SST for each segment and its respective 90-day running mean centered at the day of observation. Upwelling events were singled out when TSM anomalies were equal or smaller than  $-1^{\circ}\text{C}$ , as advocated by the existing literature (Aguiar et al. 2014).

### 3. Results and Discussion

Method 1 identified 47 upwelling events, whereas Methods 2 and 3 detected 34 and 25 events, respectively (Figure 2). The most intense upwelling events, which are characterized by the highest negative SST anomalies, occurred in segment 3 and for all 3 methods M1, M2 and M3. Highest negative anomalies were recorded on two occasions: on 12/26/2004, when anomalies were  $-2.7^{\circ}\text{C}$  (M1),  $-2.2^{\circ}\text{C}$  (M2) and  $-2.6^{\circ}\text{C}$  (M3), and on 03/17/2012 when anomalies were  $-2.5^{\circ}\text{C}$  (M1) and  $-2.1^{\circ}\text{C}$  (M2). In addition, segment 3 is linked with the highest mean negative SST anomalies, which were  $-1.5^{\circ}\text{C}$  (M1) and  $-1.3^{\circ}\text{C}$  (M2 and M3). The smallest negative SST anomalies were found in segment 6 for M1 and M2 ( $-1.2^{\circ}\text{C}$ ), while the smallest negative SST anomaly for M3 occurred in segment 9 ( $-1.1^{\circ}\text{C}$ ). Averaged negative SST anomalies of  $-1.4^{\circ}\text{C}$  (M1) and  $-1.3^{\circ}\text{C}$  (M2 and M3) were observed over the region of study.

The great majority of the events occurred between November and March, with the largest frequencies on December and March. The upwelling was most frequent in segments 1 to 4 for all of the three methods, and Method 2 identified the largest number of events between segments 5 and 9. Among the three methods used to identify the upwelling events, method M1 (that subtracts the image average SST from the segment mean) was the most sensitive in the segments to the north of BTS. This suggests that the shelf in this region is the coolest area in the whole image, and is apparently permanently cooled during austral summer. The summer month-mean temperatures of segments 1-4 are the lowest on the shelf, with mean temperatures  $0.5^{\circ}\text{C}$  lower than image average.

Methods M2 and M3, by using as a reference either the climatological SST or the 90-day running mean SST of the respective segment, can only identify strong upwelling events. This is because the reference SST is biased by the seasonal cycle that already includes upwelling events (M2) and sometimes cool water events that last for a longer period (M3). Therefore, M2 and M3 anomalies are smaller than M1 anomalies. M2 and M3 are also more sensitive in segments 6 to 9, which is explained by i) their elevated climatological mean temperature in the austral spring and summer when compared to the entire region, and by ii) the fact that the anomaly is calculated with temperature data from each segment. Hence, even if the temperature on the shelf is higher than that in the ocean, local temperature variations may result in negative anomalies.

Overall, the upwelling events reported here covered the whole continental shelf and extended offshore as far as 50 km beyond the shelf break. Fig. 3a shows the histogram of 4 size-classes of upwelled plumes in the study region along with their characteristic spatial surface coverage. All three methods (M1, M2 and M3) show an overlap of the 4 different class-size plumes in segments 3 and 4, suggesting a hot spot for the phenomenon. The majority of the surface plumes had an area smaller than  $2000\text{ km}^2$ , where 44% of them were smaller than  $1000\text{ km}^2$ . The average surface areas of each of the four class-sizes were  $593\text{ km}^2$ ,  $1388\text{ km}^2$ ,  $2326\text{ km}^2$  and  $4041\text{ km}^2$ , respectively. The largest plume (February 3rd 2008) was  $5,625\text{ km}^2$ , which covered 50% of the study region ( $11.125\text{ km}^2$ ). Furthermore, upwelled waters were recorded inside the BTS on 19 events, reaching 17 km inland. The tidal excursion in the BTS was approximately 10 km during spring tides.

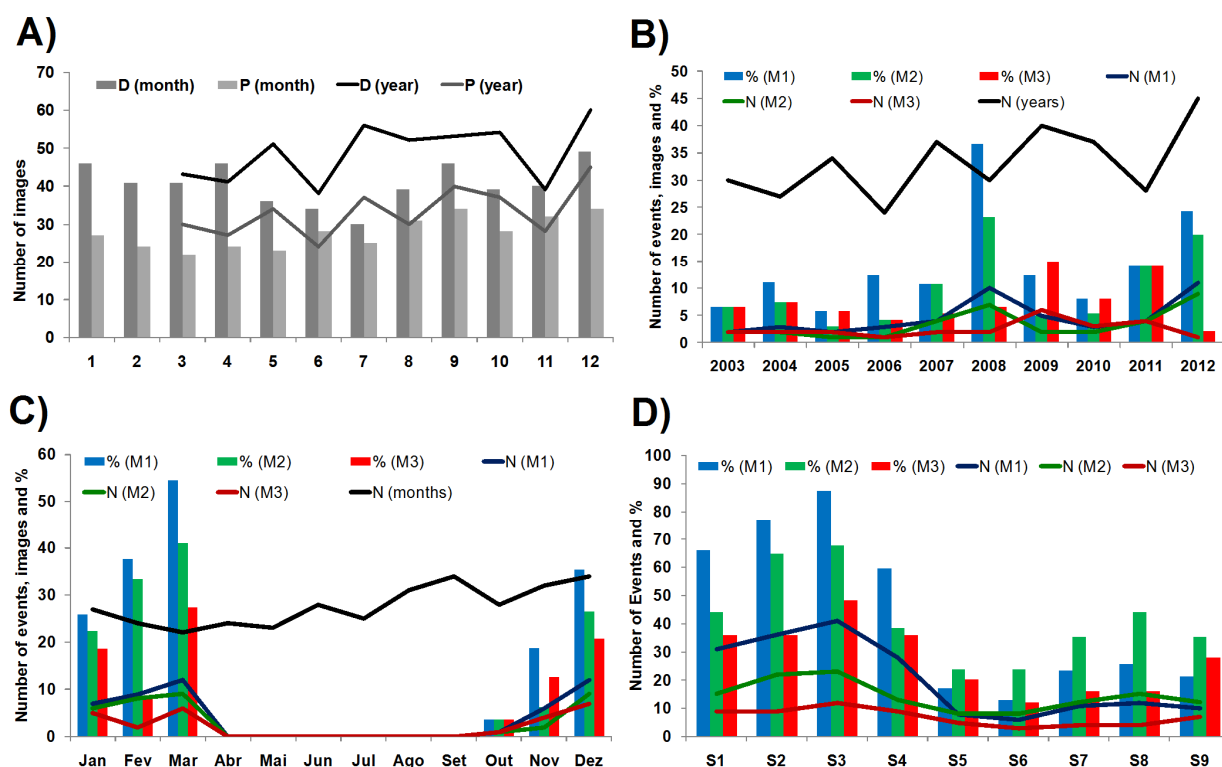


Figure 2: A) Number of images downloaded (D - thick line) and processed (P - thin line) per year and per month (bars); B) Total number of processed images (N) per year (black line), number of events identified per method (colored lines) and percentage of events relative to the total number of images per year (bars). C) Number of events (colored lines), total number of processed images per month (black line) and percentage of events relative to the total number of images per month (bars); D) Number of events per segment (lines) and percentage of events relative to the total number of events identified by each method (bars).

The smaller negative SST anomalies in the north is also consistent with the smaller dimensions of the upwelled plumes. The spatial surface magnitude of the largest upwelling event in Cabo Frio was 33,880 km<sup>2</sup> (Figure 3b), with a maximum extension of 2.5° of latitude (~250 km) and 4.6° of longitude (~460 km). In this study, the largest plume identified was 5,279 km<sup>2</sup> in area (Figure 3c), with a maximum horizontal extension of 1.4° of latitude (~138 km) and 0.7° of longitude (~72 km). The temporal extent of the events, as indicated by sequential images, varied between 72 hours and 120 hours. However, the sensors deployed inside the BTS indicate that negative temperature anomalies can last up to 11 days.

Previous studies have shown the close association between negative SST anomalies and positive Chla concentration anomalies, such as Kampel (2003) at Cabo Frio and Oke and Middleton (2000) in Australia. Chla concentrations obtained in the study area varied between 1.18 and 9.45 mgm<sup>-3</sup>, which were close to the mean and maximum Chla concentrations of 0.46 mgm<sup>-3</sup> and 11.0 mgm<sup>-3</sup> reported for Cabo Frio (Kampel, 2003). However, the peak Chla concentrations in the study area were not associated with negative SST anomalies. The results showed no correlation between negative SST and positive Chla concentration anomalies detected by methods M1 and M2, and even positive correlations (decrease of the SST anomalies and increase in Chla) have been observed in the southern segments (6, 8 and 9). The best correlation coefficients were 0.50 (segment 1) and 0.44 (segments 1 and 3), respectively, for M1 and M2. Slightly better correlations were obtained for method M3, which resulted in R<sup>2</sup> of -0.90 at segment 5.

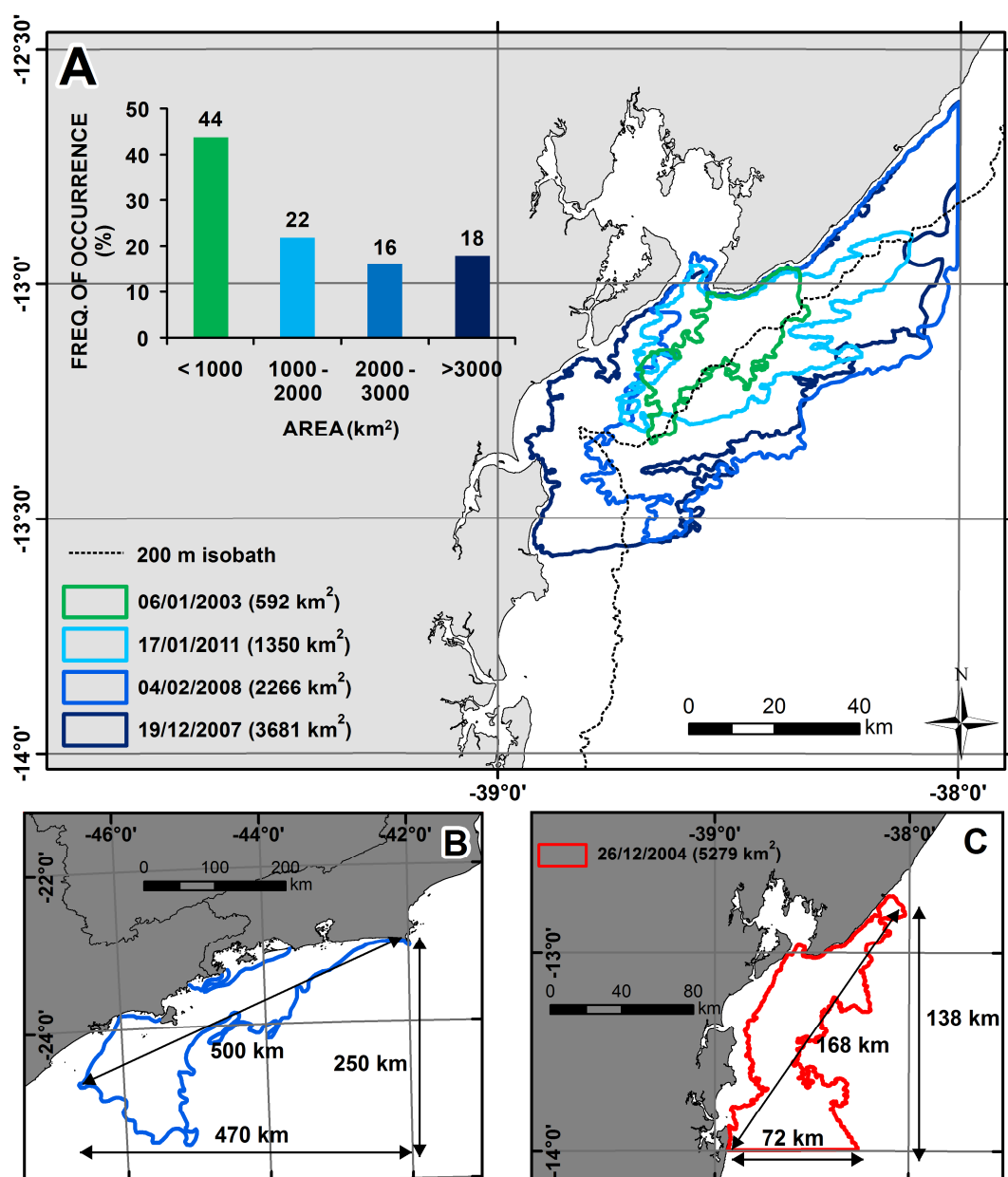


Figure 3: Map with the perimeter of 4 upwelling events characteristic of each plume-area class in the histogram. b) Map of the Rio de Janeiro Coast showing the dimensions of the largest upwelled plume on October 4<sup>th</sup> 2001 (adapted from Mello-Filho, 2006) e c) Dimensions of the largest upwelled plume in the study area on December 26<sup>th</sup> 2004.

The poor correlation between the SST and Chla concentration anomalies maybe due to: i) few sequential satellite images, ii) Chla signals produced by the outflow of the coastal bays and, especially, sewage outfalls, and iii) similar Chla concentrations throughout the upwelled water column (100 m of depth). The lack of information on the developmental stage of the detected upwelling implies that the measured Chla concentrations may not have yet responded to changes in nutrient levels (Kim et al., 2007), *i.e.*, time lags cannot be accounted for. Bays, rivers and sewage outflows add an extra amount of nutrients to the coast, and can locally increase the Chla concentrations. In the study region, apart from BTS, there are several streams draining densely urbanized areas that flow directly to the ocean.



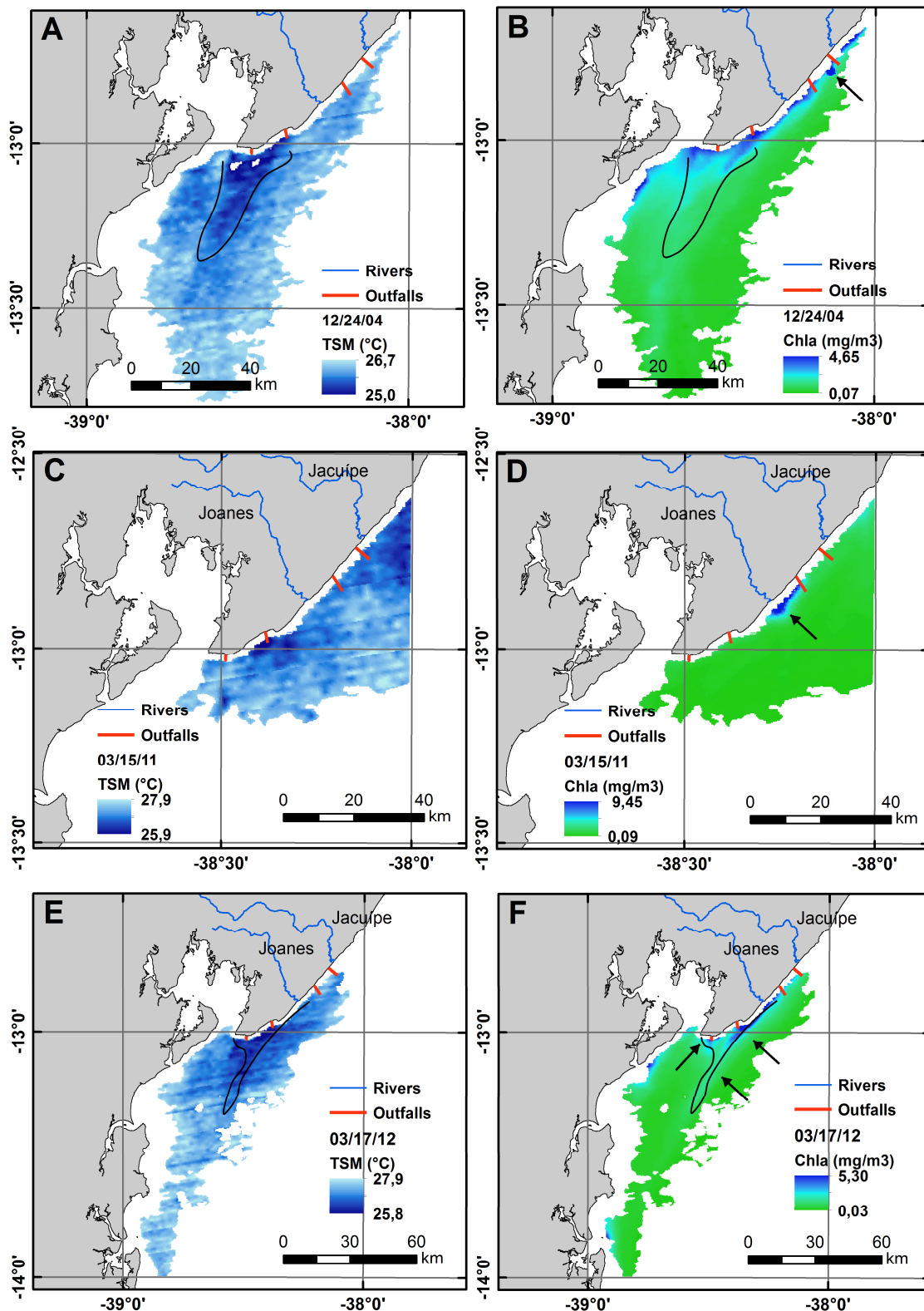


Figure 4: SST (left panels) and Chla concentrations (right panels) for a, b) December 24 2004, c, d) March 15 2011 and e, f) March 17 2012. The black line delimits the upwelled plume. The outfalls, from south to north, are named Rio Vermelho, Jaguaribe, Cristal and Cetrel.

These outflows occur at two sewage (Jaguaribe and Rio Vermelho) and two industrial (Cristal and CETREL) outfalls, as well as at two rivers (Joanes and Jacuípe) with mean annual discharges bigger than  $10 \text{ m}^3 \text{ s}^{-1}$ . Figure 4 shows examples of high Chla concentrations

associated with the sewage outfalls that bias the spatial correlation between Chla and SST anomalies. On 12/24/04 (Figure 4a-b), the highest Chla concentrations are far away from the upwelled plume, and instead are located close to Cristal's outfall (black arrow). On 03/15/11 (Figure 4c-d) higher Chla concentrations can be traced again to Cristal's outfall. Finally on 03/17/12 (Figure 4e-f), an area with high Chla associated with the Joanes River and Rio Vermelho outfalls coincided with the plume's perimeter.

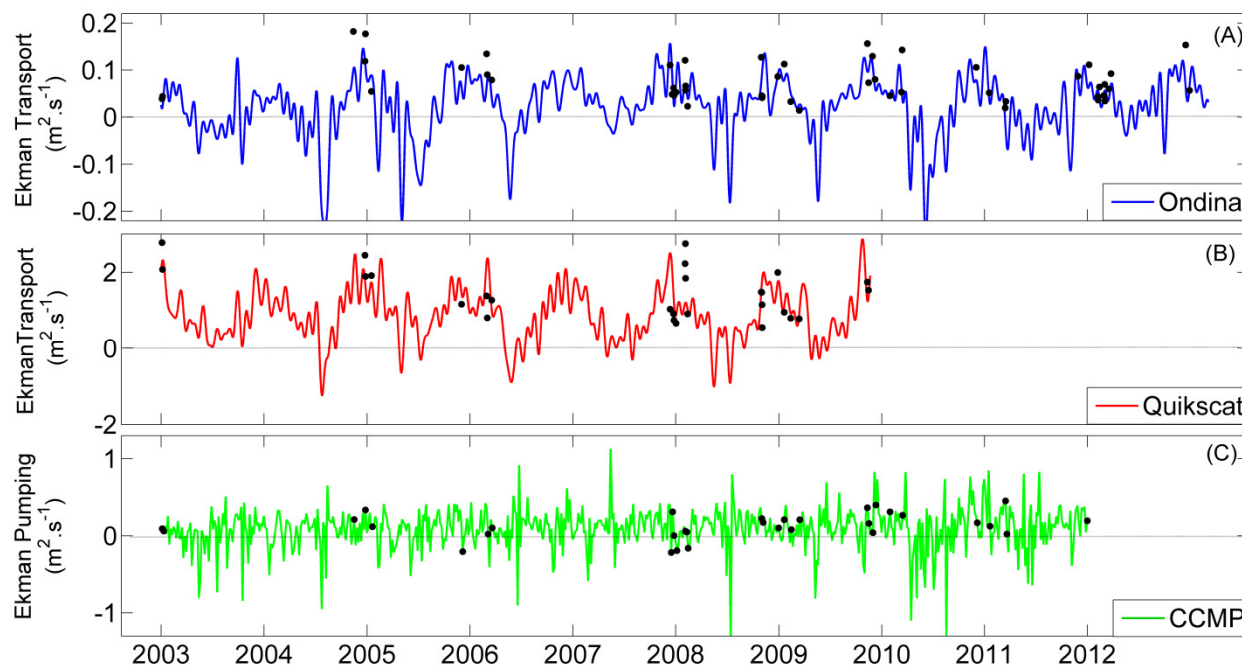


Figure 5: Ekman transport and its 72 hours mean preceding each upwelling event (black dots), calculated with Ondina (A), QuikSCAT (B) wind data and Ekman Pumping and its 5 day average (C).

The wind has been considered as the main forcing agent for upwelling on the Brazilian coast (Aguiar et al., 2014; Castro and Miranda, 1998; Campos et al., 2013). Their results indicate a high correlation between the intensification of NE winds and the development of negative SST anomalies. The climatology of the alongshore wind component from the INMET station and QuikSCAT in this study correlates well and is consistent with the seasonality of the upwelling events reported here. The 72-hour mean  $T_{EK}$  values preceding the upwelling events are generally positive, varying from  $0.01 \text{ m}^2 \text{ s}^{-1}$  to  $0.18 \text{ m}^2 \text{ s}^{-1}$  based on INMET's winds (Figure 5a), and  $0.56 \text{ m}^2 \text{ s}^{-1}$  to  $3.47 \text{ m}^2 \text{ s}^{-1}$  based on QuikSCAT's winds (Figure 5b). In addition, with the exception of four events, all events between 2003 and 2011 (Figure 5c) had positive  $T_{PUMP}$ , which reached a maximum of  $0.45 \text{ m}^2 \text{ s}^{-1}$ . Transport values calculated by Aguiar et al. (2014) presented the same seasonal trend (largest transport between September and April) and the same magnitude. The  $T_{EK}$  calculated around Prado ( $17.1^\circ\text{S}$ ), varied between  $-0.5 \text{ m}^2 \text{ s}^{-1}$  and  $1.6 \text{ m}^2 \text{ s}^{-1}$  between the winter and the summer.

A few of the detected upwelling events occurred under unfavorable or only slightly favorable wind conditions, suggesting that other forcing mechanisms can also play a role in the upwelling events. Rodrigues and Lorenzetti (2001) point out that changes in the orientation of the continental margin and in the bathymetry are factors of relevance to the development of coastal upwelling. Palma and Matano (2009) also argue that geometric changes (width and orientation) of the continental shelf create a negative meridional pressure gradient that transports upper-slope water onto the shelf. A numerical model-based investigation on the Cabo de São Tomé upwelling by Palocz et al. (2014) indicated that the

winds play a central role in the region, but that meanders are also very important in 61% of the recorded events.

#### 4. Conclusions

In this study, three methods for calculating negative SST anomalies in daily SST images allowed the identification of 50 upwelling events. *In situ* water temperature data at the entrance of the BTS showed a consistent cooling of the entire water column during the events. Results obtained here show that upwelling was more frequent between November and March, might persist for up to 11 days. The largest mapped upwelled plume was 5,279 km<sup>2</sup>, extending offshore as far as 50 km beyond the shelf break.

Results obtained here suggest that the 24°C isotherm may be used as a proxy for the upwelled waters in the study area. This temperature is characteristic of the Tropical Water between 50 and 100 m of depth, which is a nutrient poor water mass. Therefore, the correlation between SST and Chla anomalies was poor, with high Chla concentrations normally observed close to sewage outfalls and river mouths. Northeast winds inducing upwelling-favorable Ekman transport and pumping were associated with all events, with the exception of 4 events where only  $T_{PUMP}$  was negative.

#### Acknowledgement

Felipe M. Santos was supported by FAPESB scholarship. Mauro Cirano was supported by CNPq Research grant. Ricardo Domingues acknowledges support from the NOAA Atlantic Oceanographic and Meteorological Laboratory. The authors would like to thank NASA and IFREMER for providing satellite data used in this paper. This work was aided by FAPESB Research Grant PET0036/2012 (Edital Baías da Bahia).

#### References

- Aguiar, A.L.; Cirano, M.; Pereira, J.; Marta-Almeida, M. Upwelling processes along a western boundary current in the Abrolhos - Campos region of Brazil. **Continental Shelf Research**, v. 85, pp. 42-59, 2014.
- Brown, O.B.; Minnett, P.J. MODIS Infrared Sea Surface Temperature Algorithm. **Algorithm Theoretical Basis Document, Version 2.0**, with contributions from: Evans, R., Kearns, E., Kilpatrick, K., Kumar, A., Sikorski, R., Závody, A. University of Miami, Miami, 1999, 98 p.
- Campos, P.C.; Moller Jr, O.O.; Piola, A.R.; Palma, E.D. Seasonal variability and coastal upwelling near Cape Santa Marta (Brazil). **J. Geophys. Res. Oceans**, v. 118, doi:10.1002/2012JC008492, 2013.
- Castro, B.M.; Miranda, L.B. Physical Oceanography of the Western Atlantic continental shelf located between 4°N and 34°S. **The Sea**, Wiley, New York, v. 11, p. 209-251, 1998.
- Kampel, M. **Estimativa da produção primária e biomassa fitoplancônica através de sensoriamento remoto da cor do oceano e dados *in situ* na costa sudeste brasileira**. Tese de Doutorado, Instituto Oceanográfico, USP, São Paulo, 279 p. 2003.
- Kim, H.C.; Yoo, S.; Sang Oh, I. Relationship between phytoplankton bloom and windstress in the sub-polar frontal area of the Japan/East Sea. **Journal of Marine Systems**, 67, 205–216, 2007.
- Mello Filho, W.L. **Observações de feições oceanográficas de superfície na costa sudeste brasileira através de imagens termais do sensor AVHRR/NOAA**. Dissertação de Mestrado em Sensoriamento Remoto, Instituto Nacional de Pesquisas Espaciais (INPE), 85 p. 2006.
- Oke, P.R., Middleton, J.H., 2000. Topographically induced upwelling off Eastern Australia. **Journal of Physical Oceanography**, v.30, p.512–531, 2000.
- O'Reilly, J.E., et al. SeaWiFS Post launch Calibration and Validation Analyses, Part 3. **NASA Tech**, Eds: Hooker S.B., Firestone, E.R., NASA Goddard Space Flight Center, 11, p. 49. 2000.
- Palma, E.D.; Matano, R.P. Disentangling the upwelling mechanisms of South Brazil Bight. **Continental Shelf Research**, v. 29, p. 1525-1534, 2009.
- Palóczy, A., Silveira, I.C.A., Castro, B.M., Calado, L. Coastal upwelling off Cape São Tomé (22°S, Brazil): The supporting role of deep ocean processes. **Continental Shelf Research**, v. 89, p. 38-50, 2014.
- Rodrigues, R.R., Lorenzetti, J.A., 2001. Numerical study of the effects of bottom topography and coastline geometry on the southeast Brazilian coastal upwelling. **Continental Shelf Research**, v. 21, p. 371–394.